



HAL
open science

A Langevin equation for turbulent velocity increments

Philippe Marcq, Antoine Naert

► **To cite this version:**

Philippe Marcq, Antoine Naert. A Langevin equation for turbulent velocity increments. *Physics of Fluids*, 2001, 13 (9), pp.2590. 10.1063/1.1386937 . hal-01140942

HAL Id: hal-01140942

<https://hal.science/hal-01140942>

Submitted on 11 Apr 2015

HAL is a multi-disciplinary open access archive for the deposit and dissemination of scientific research documents, whether they are published or not. The documents may come from teaching and research institutions in France or abroad, or from public or private research centers.

L'archive ouverte pluridisciplinaire **HAL**, est destinée au dépôt et à la diffusion de documents scientifiques de niveau recherche, publiés ou non, émanant des établissements d'enseignement et de recherche français ou étrangers, des laboratoires publics ou privés.

A Langevin equation for turbulent velocity increments

Philippe Marcq and Antoine Naert

Citation: *Physics of Fluids* (1994-present) **13**, 2590 (2001); doi: 10.1063/1.1386937

View online: <http://dx.doi.org/10.1063/1.1386937>

View Table of Contents: <http://scitation.aip.org/content/aip/journal/pof2/13/9?ver=pdfcov>

Published by the [AIP Publishing](#)

Articles you may be interested in

[Gaussian approximations for stochastic systems with delay: Chemical Langevin equation and application to a Brusselator system](#)

J. Chem. Phys. **140**, 124112 (2014); 10.1063/1.4867786

[Conditional Eulerian and Lagrangian velocity increment statistics of fully developed turbulent flow](#)

Phys. Fluids **23**, 055102 (2011); 10.1063/1.3584123

[Conditional statistics for passive-scalar mixing in a confined rectangular turbulent jet](#)

Phys. Fluids **19**, 055104 (2007); 10.1063/1.2718580

[Anomalous scaling exponents and coherent structures in high Re fluid turbulence](#)

Phys. Fluids **12**, 676 (2000); 10.1063/1.870273

[Quadratic Markov modeling for intermittent turbulence](#)

Phys. Fluids **11**, 1694 (1999); 10.1063/1.870034



A Langevin equation for turbulent velocity increments

Philippe Marcq^{a)}

Institut für Physik, Universität Potsdam, D-14415 Potsdam, Germany

Antoine Naert

Laboratoire de Physique, École Normale Supérieure de Lyon, 46 Allée d'Italie, 69364 Lyon Cédex 07, France

(Received 22 November 1999; accepted 1 June 2001)

Recently, Friedrich and Peinke demonstrated empirically that a Fokker–Planck equation describes the scale dependence of probability distribution functions of longitudinal velocity increments v_r in fully developed turbulent flows. Thanks to the analysis of an experimental velocity signal, the stochastic process v_r is further investigated by examining the related Langevin equation. This process is found to be Markovian in scale because the turbulent velocity field is correlated over distances much larger than the correlation length ρ of its spatial derivative. A Gaussian approximation for the random force yields evolution equations for the structure functions $\langle v_r^n \rangle$. Analytic solutions are obtained, in agreement with experimental data for even-order moments when the scale r is larger than a few times ρ . The third-order moment $\langle v_r^3 \rangle$ is found linear in r , as predicted by Kolmogorov's four-fifths law. © 2001 American Institute of Physics.
[DOI: 10.1063/1.1386937]

I. INTRODUCTION

The physics of high Reynolds number, incompressible hydrodynamic flows remains poorly understood. One important characterization is the probability distribution function (*pdf*) $P(v_r, r)$ of longitudinal velocity increments v_r at scale r , an experimentally measurable quantity. At high enough Reynolds number, and for intermediate (inertial) scales, i.e., sufficiently far from the energy injection and dissipation scales, Kolmogorov's scaling hypothesis¹ states that $P(v_r, r)$ becomes a universal function of the ratio $v_r / (\langle \epsilon \rangle r)^{1/3}$, where $\langle \epsilon \rangle$ denotes the mean energy dissipation rate of the flow. An important goal of current research on fully developed turbulence is to quantify and understand the deviations from Kolmogorov's scaling observed at experimentally accessible Reynolds numbers.² Approximately Gaussian at large scale, the distribution $P(v_r, r)$ progressively develops long tails toward small scales, due to the presence in the flow of tiny regions of very high shear and dissipation. It is also known that $P(v_r, r)$ is slightly asymmetric, as characterized in the inertial range by Kolmogorov's four-fifths law $\langle v_r^3 \rangle = -(4/5)\langle \epsilon \rangle r^1$.

Recent work on experimental velocity signals indicates that $P(v_r, r)$ is the solution of a Fokker–Planck equation.³ The velocity increment v_r is therefore well described by a continuous stochastic process in scale, *Markovian* for large enough scales where viscous effects are negligible.⁴ This proves that the turbulent cascade process is local in scale. Moreover, theoretical work has shown that a Fokker–Planck equation for $P(v_r, r)$ can be derived, thanks to field-

theoretical techniques, from the Navier–Stokes equation with random forcing.⁵

The goal of this article is to further investigate the stochastic process v_r by studying the stochastic differential equation which governs its trajectories in scale. This study closely follows a similar investigation of a Langevin equation for the energy dissipation field of fully developed turbulent flows:⁶ coefficients of the Langevin equation for v_r are evaluated directly from experimental data (Sec. III). One benefit is immediate access to the stochastic term of the equation. We give a physical interpretation of the Markovian character of v_r (Sec. IV), and show that this approach yields a quantitatively accurate description of the random process. A Gaussian approximation of the random force allows one to compute analytically the scale dependence of the structure functions $\langle v_r^n \rangle$ (Sec. V).

II. EXPERIMENT

The turbulent flow studied in this article is an axisymmetric jet in air.⁷ Time series of the longitudinal velocity component $u(x_0, t)$ are recorded by hot-wire anemometry at a single point x_0 on the jet axis. The velocity probe is placed 2 m downstream from the nozzle, sufficiently far (40 times the nozzle's diameter) for the turbulence to be considered locally homogeneous and isotropic. The hot wire is a TSI 1210-T1.5 tungsten wire of diameter $d_w = 4 \mu\text{m}$ and sensing length $1.24 \text{ mm} = 310d_w$, controlled by an IFA 100 anemometer operated at constant temperature 250 °C. The output signal is low-pass filtered at a cutoff frequency f_c , then sampled at a frequency $f_s = 39 \text{ kHz} \approx 2f_c$ (in practice $f_c \approx \langle u \rangle / \eta$, where η is Kolmogorov's scale), then digitized with a 23 bit analog-to-digital converter on an HP E1430A workstation.

^{a)}Permanent address: IRPHE—Université de Provence, 49, rue Joliot-Curie, 13384 Marseille, Cedex 13, France; electronic mail: Philippe.Marcq@irphe.univ-mrs.fr

The high turbulence intensity observed in this flow ($u_{\text{rms}}/\langle u \rangle \approx 28\%$) means that Taylor’s “frozen turbulence hypothesis” fails when turning the recorded time series $u(x_0, t = t_0 + \Delta t)$ into spatial measurements: $u(x = x_0 - \langle u \rangle \Delta t, t_0) \neq u(x_0, t_0 + \Delta t)$. Indeed, recording the velocity at constant sampling frequency gives rise to a *statistical bias* when fluctuations are important, i.e., at high values of the turbulence intensity. A slowly evolving part of the velocity field will be over-sampled, i.e., over-represented in the statistics. On the contrary, a fast part of the signal will be under-represented. This bias becomes larger at higher values of the fluctuation rate. Following Ref. 8 we choose to correct this bias by regularly resampling the data. Denoting the recorded time series by $\{u_j\}_{j=0, \dots, N}$, we first construct an “abscissa signal” $x_j = ju_j$, then divide it into N intervals $[\hat{x}_j, \hat{x}_{j+1}]$ of equal length ($\hat{x}_0 = x_0, \hat{x}_N = x_N$). Values of the de-biased velocity signal \hat{u}_j are obtained by linear interpolation at the new position $\hat{x}_j, \hat{u}_j = u(\hat{x}_j)$. We checked that using a higher-order interpolation scheme yields the same velocity field. In the following, the *spatial* velocity field is denoted $u(x_j) = \hat{u}_j$ for simplicity.

Longitudinal (de-biased) velocity increments are defined as $v_r(x) = u(x+r) - u(x)$, where r is the separation scale. Ergodicity is assumed to be valid: ensemble averages (denoted by $\langle \rangle$) are computed as averages over x (at fixed r). The mean and rms velocity are, respectively, $\langle u \rangle = 3.3 \text{ m s}^{-1}$ and $u_{\text{rms}} = 0.9 \text{ m s}^{-1}$. The mean energy dissipation rate $\langle \epsilon \rangle$ is evaluated from the small-scale behavior of the second-order structure function $\langle v_r^2 \rangle$:

$$\langle \epsilon \rangle = \lim_{r \rightarrow 0} \frac{15\nu}{r} \frac{\partial}{\partial r} \langle v_r^2 \rangle. \quad (1)$$

We find $\langle \epsilon \rangle = 3.5(1) \text{ m}^2 \text{ s}^{-3}$. Kolmogorov’s dissipation scale and Taylor’s microscale are, respectively, $\eta \approx 175 \mu\text{m}$ and $\lambda = 7 \text{ mm} \approx 40\eta$. The microscale Reynolds number is $R_\lambda \approx 430$. The third-order structure function $\langle v_r^3 \rangle$ is approximately linear in r (*inertial-range* scaling) over one decade of scales: $40\eta \leq r \leq 400\eta$ (see Fig. 4).

The integral scale is defined as the sum $L = \int_0^\infty C_u(r) dr$ of the normalized velocity autocorrelation function $C_u(r) = \langle u(x)u(x+r) \rangle / \langle u^2 \rangle$. We find $L = 14 \text{ cm} \approx 800\eta$. We use a sample of 14×10^7 points ($9 \times 10^5 L$), long enough to ensure that all statistical quantifiers have converged. Similar results are obtained for other data sets corresponding to other Reynolds numbers.

III. LANGEVIN EQUATION

The goal of this section is to evaluate the parameters of the Langevin equation:

$$-\frac{dv_r}{dr} = D_1(v_r, r) + \sqrt{2D_2(v_r, r)} \xi(r), \quad (2)$$

assumed to describe the scale dynamics of the stochastic process v_r . The minus sign on the left-hand side reflects the physical direction of the turbulent cascade from large (injection) to small (dissipation) scales. One realization of $v_r(x) = u(x+r) - u(x)$ corresponds to a fixed value of the position x , while r varies within the bounded interval: $L \geq r \geq \eta$. The

variable x is generally omitted to make notations simpler. We checked that similar results are obtained for centered velocity increments $v_r(x) = u(x+r/2) - u(x-r/2)$.

The random force $\xi(r)$ must respect $\langle \xi(r) \rangle = 0$ and $\langle \xi(r)^2 \rangle = 1$ at all scales.⁹ The drift and diffusion coefficients $D_1(v_r, r)$ and $D_2(v_r, r)$ are therefore equal to

$$D_1(v_r, r) = - \left\langle \frac{dv_r}{dr} \middle| v_r \right\rangle, \quad (3)$$

$$D_2(v_r, r) = \frac{1}{2} \left\langle \left(\frac{dv_r}{dr} + D_1(v_r, r) \right)^2 \middle| v_r \right\rangle, \quad (4)$$

where $\langle f(v_r, r) | v_r \rangle$ denotes the conditional average of the function $f(u, r)$ at a fixed value v_r of u : $\langle f(v_r, r) | v_r \rangle = \langle f(u, r) | u = v_r \rangle$.

In practice, Ito’s conventions for stochastic calculus are used when evaluating the derivative dv_r/dr .⁹ This yields the following discrete equation ($\delta r > 0$):

$$v_r = v_{r+\delta r} + D_1(v_r, r) \delta r + \sqrt{2D_2(v_r, r)} \delta r \xi(r). \quad (5)$$

The derivative dv_r/dr is correctly described by Eq. (5) when the discrete step δr is smaller than η , i.e., for scales below which v_r is smooth. We use the value $\delta r = \eta/2$ hereafter, equivalent to one sampling step. The drift coefficient is evaluated as $D_1(v_r, r) = \langle v_r - v_{r+\delta r} | v_r \rangle / \delta r$. We find that D_1 is a linear function of v_r when $50\eta \leq r \leq L$:

$$D_1(v_r, r) = -\gamma \frac{v_r}{r}, \quad (6)$$

where $\gamma \approx 1/3$ [see Fig. 1(a)]. According to Eq. (5), the diffusion coefficient is equal to the following conditional average:

$$D_2(v_r, r) = \frac{1}{2\delta r} \langle (v_r - v_{r+\delta r} - D_1(v_r, r) \delta r)^2 | v_r \rangle. \quad (7)$$

Its unit is therefore m s^{-2} [see also Eq. (11)]. We find that D_2 is well fitted by a cubic function of v_r for scales larger than 50η [Fig. 1(b)]:

$$D_2(v_r, r) = d_0 - d_1 v_r + d_2 \frac{v_r^2}{r} + d_3 \frac{v_r^3}{r}, \quad (8)$$

where $d_0 = 0.56 \pm 0.06 \text{ m s}^{-2}$, $d_1 = 0.045 \pm 0.015 \text{ s}^{-1}$, $d_2 = 0.0057 \pm 0.0002$, and $d_3 = 0.0015 \pm 0.0002 \text{ m}^{-1} \text{ s}$

Values of the first- and second-order Kramers–Moyal coefficients, estimated as in Ref. 3, are consistent with Eqs. (6) and (8), albeit with a somewhat poorer accuracy. The asymmetry observed here for $D_2(d_1, d_3 \neq 0)$ is indeed apparent in the figures of Ref. 3. However, the diffusion coefficient of the Fokker–Planck equation predicted by Ref. 5 is *quadratic* (i.e., $d_3 = 0$ in our notations), with $D_2(0, r) = 0 (d_0 = 0)$, at odds with experimental data.

The (dimensionless) random force $\xi(r)$ can now be evaluated as

$$\xi(r) = - \frac{v_r - v_{r+\delta r} - D_1(v_r, r) \delta r}{\sqrt{2D_2(v_r, r)} \delta r}. \quad (9)$$

For consistency, we checked that $\langle \xi(r) \rangle \approx 0 (|\langle \xi(r) \rangle| \leq 10^{-4})$ and $\langle \xi(r)^2 \rangle \approx 1 (|\langle \xi(r)^2 \rangle - 1| \leq 10^{-3})$, and find for

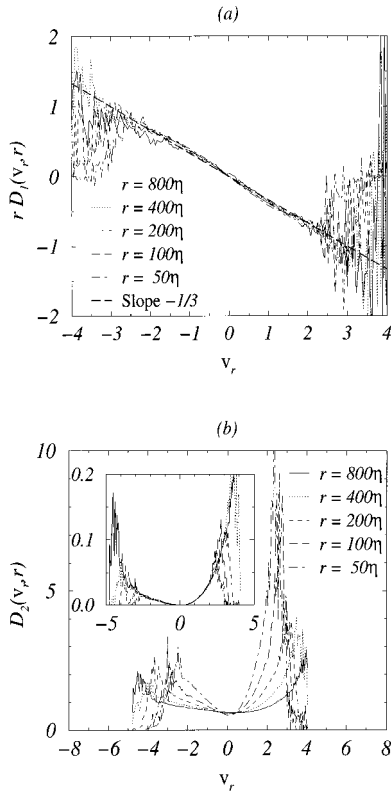


FIG. 1. (a) Drift coefficient $D_1(v_r, r)$. The slope of $rD_1(v_r, r)$ vs v_r is consistent with $-1/3(D_1(v_r, r) \approx -\frac{1}{3}v_r/r)$. Both $rD_1(v_r, r)$ and v_r are given in m s^{-1} . (b) Diffusion coefficient $D_2(v_r, r)$ (unit: m s^{-2}) vs v_r (unit: m s^{-1}). Inset: $r(D_2(v_r, r) - d_0 + d_1v_r)$ is well fitted by $d_2v_r^2 + d_3v_r^3$ ($d_0 = 0.56 \text{ m s}^{-2}$, $d_1 = 0.045 \text{ s}^{-1}$, $d_2 = 0.0057$; $d_3 = 0.0015 \text{ m}^{-1} \text{ s}$). The drift and diffusion coefficients are given for scales r between 50η and $L = 800\eta$.

scales larger than 50η that $\langle v_r \xi(r) \rangle \approx 0$ within statistical error ($\langle v_r \xi(r) \rangle \leq 10^{-3} \langle v_r^2 \rangle^{1/2}$). The pdf $P(\xi, r)$ is shown in Fig. 2(a). It does not depend on scale. Two characteristic features of $P(\xi, r)$ are its asymmetry (skewness coefficient $S(\xi) = \langle \xi^3 \rangle / \langle \xi^2 \rangle^{3/2} \approx 0.55$) and the presence of long tails [flatness coefficient $F(\xi) = \langle \xi^4 \rangle / \langle \xi^2 \rangle^2 \approx 8.5$].

IV. A MARKOVIAN PROCESS

The stochastic process defined by Eq. (2) is Markovian if the random force $\xi(r)$ is correlated over a range of scales much smaller than the autocorrelation scale of the variable v_r . Figure 2(b) shows that this is indeed the case: The autocorrelation function of $\xi(r)$, defined as $C_\xi(r, \Delta r) = \langle \xi(r)\xi(r+\Delta r) \rangle$, decays rapidly. Its (r -independent) autocorrelation scale ρ , defined for instance by the integral $\rho = \int_0^\infty C_\xi(r, \Delta r) d\Delta r$, is small compared to the autocorrelation scale of v_r (and u): $\rho \approx 8\eta \ll L \approx 800\eta$. In practice, this suggests that $C_\xi(r, \Delta r)$ can be safely approximated by a δ function for scales large compared to ρ , e.g., in the inertial range.

The scale derivative dv_r/dr at position x is in fact equal to the spatial derivative du/dx computed at position $x+r$: since $dv_r/dr \approx (v_{r+h} - v_r)/h$, where $h \ll r$, we have

$$\frac{dv_r}{dr} \approx \frac{1}{h}(u(x+r+h) - u(x+r)) \approx \frac{du}{dx}(x+r). \quad (10)$$

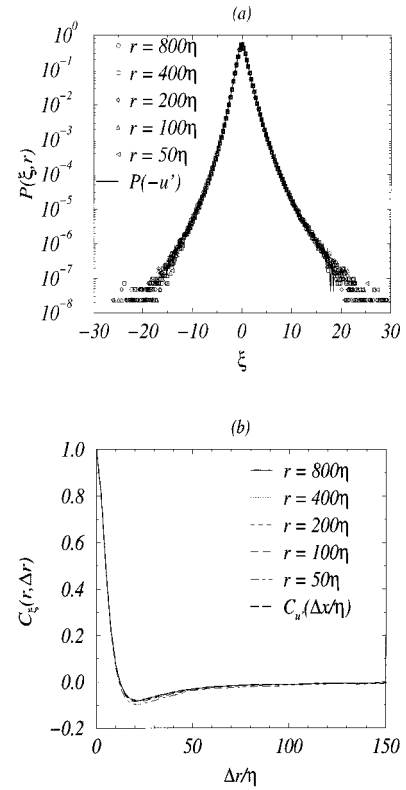


FIG. 2. (a) The probability distribution functions of the random force $\xi(r)$ ($\langle \xi(r)^2 \rangle = 1$) are independent of scale for scales r between 50η and $L = 800\eta$, and identical to the pdf $P(-u')$ of the opposite of the (normalized) velocity derivative $u' = (du/dx) / \langle (du/dx)^2 \rangle^{1/2}$. The random force $\xi(r)$ is dimensionless. (b) The autocorrelation functions $C_\xi(r, \Delta r)$ of the random force $\xi(r)$ are plotted vs the dimensionless scale increment $\Delta r/\eta$ in the same range of scales $50\eta \leq r \leq 800\eta$. A plot of the autocorrelation function $C_u(\Delta x)$ of u' vs the dimensionless spatial increment $\Delta x/\eta$ is given for comparison.

The random force $\xi(r)|_x$ defined by Eq. (9) is therefore a linear function of the velocity derivative $du/dx|_{x+r}$. We have checked that the normalized cross-correlation coefficient $\langle \xi(r)|_x du/dx|_{x+r} \rangle / \langle (du/dx)^2 \rangle^{1/2}$ is indeed close to -1 in the inertial range. Figure 2 confirms that $\xi(r)$ and $-du/dx$ are statistically equivalent: The normalized autocorrelation functions of the two variables are identical; the skewness and flatness coefficients of the random force are equal to $S(\xi) = -S(du/dx)$ and $F(\xi) = F(du/dx)$.

In other words, the velocity increment v_r is Markovian in r because the velocity $u(x)$ is correlated over distances much larger than the correlation length of its derivative du/dx . [A similar argument⁶ shows that the averaged dissipation ϵ_r is also a Markovian process in r since its correlation scale is much larger than the correlation length of the local dissipation $(du/dx)^2$.]

V. A GAUSSIAN APPROXIMATION

A. Evolution equations for the moments of velocity increments

We assumed in Sec. III that the disordered trajectories in scale of the variable v_r can be described by a stochastic differential equation [Eq. (2)]. Using this equation, we pro-

ceeded to evaluate this equation’s drift and diffusion coefficients [Eqs. (3) and (7)] and random force [Eq. (9)] from an experimental velocity signal. In Sec. IV, we verified that the noise variable $\xi(r)$ is indeed a “fast” variable compared to the “slow” v_r , as implicitly assumed in (2).

The goal of this section is to test the validity of Eq. (2). Since the random process v_r is already known to be Markovian for large enough scales, approximating the random force $\xi(r)$ by a Gaussian process makes the Langevin equation equivalent to a Fokker–Planck equation. We will show that this Gaussian approximation yields analytical expressions of the scale dependence of the moments $\langle v_r^n \rangle$ in agreement with experimental data.

The Fokker–Planck equation reads⁹

$$-\frac{\partial}{\partial r}P(v_r, r) = -\frac{\partial}{\partial v_r}(D_1(v_r, r)P(v_r, r)) + \frac{\partial^2}{\partial v_r^2}(D_2(v_r, r)P(v_r, r)). \quad (11)$$

A hierarchy of evolution equations for the moments $\langle v_r^n \rangle$ is easily obtained from (11):

$$-\frac{d}{dr}\langle v_r^n \rangle = n\langle D_1(v_r, r)v_r^{n-1} \rangle + n(n-1)\langle D_2(v_r, r)v_r^{n-2} \rangle. \quad (12)$$

Since initial conditions are given at large scale L , natural nondimensional variables are $\bar{r} = r/L$ and $\bar{v}_r = v_r/u_{\text{rms}}$. Using the coefficients D_1 and D_2 as expressed in Eqs. (6)–(8) the nondimensional evolution equation for $\langle \bar{v}_r^n \rangle$ reads

$$\frac{d}{d\bar{r}}\langle \bar{v}_r^n \rangle = \frac{\alpha_n}{\bar{r}}\langle \bar{v}_r^n \rangle - n(n-1)\left(\bar{d}_0\langle \bar{v}_r^{n-2} \rangle - \bar{d}_1\langle \bar{v}_r^{n-1} \rangle + \frac{\bar{d}_3}{\bar{r}}\langle \bar{v}_r^{n+1} \rangle\right), \quad (13)$$

where coefficients γ , d_2 , and $\alpha_n = n(\gamma - (n-1)d_2) = \bar{\alpha}_n$ are unchanged, and

$$\bar{d}_0 = d_0L/u_{\text{rms}}^2 = 0.09 \pm 0.01, \quad (14)$$

$$\bar{d}_1 = d_1L/u_{\text{rms}} = 0.007 \pm 0.001, \quad (15)$$

$$\bar{d}_3 = d_3u_{\text{rms}} = 0.0013 \pm 0.0002. \quad (16)$$

Noting that $\gamma \approx 1/3$, Kolmogorov scaling $\langle v_r^n \rangle \propto r^{n/3}$ would be recovered for $D_2(v_r, r) = 0$.

B. Even-order moments

Let us first consider even-order moments: $n = 2p$. Since $P(v_r, r)$ is weakly asymmetric in the inertial range ($S(v_r) \approx -0.25$), the odd-order moments $|\langle \bar{v}_r^{2p-1} \rangle|$ and $|\langle \bar{v}_r^{2p+1} \rangle/\bar{r}|$ are small compared to $\langle \bar{v}_r^{2p-2} \rangle$. A good approximation of Eq. (13) thus reads ($\bar{d}_1, \bar{d}_3 \ll \bar{d}_0$)

$$\frac{d}{d\bar{r}}\langle \bar{v}_r^{2p} \rangle = \frac{\alpha_{2p}}{\bar{r}}\langle \bar{v}_r^{2p} \rangle - 2p(2p-1)\bar{d}_0\langle \bar{v}_r^{2p-2} \rangle. \quad (17)$$

The exact solution of Eq. (17) is

$$\langle \bar{v}_r^{2p} \rangle = \langle \bar{v}_{\bar{r}=1}^{2p} \rangle \bar{r}^{\alpha_{2p}} - \bar{d}_0 2p(2p-1) \bar{r}^{\alpha_{2p}} \times \int_1^{\bar{r}} \rho^{-\alpha_{2p}} \langle \bar{v}_\rho^{2p-2} \rangle d\rho. \quad (18)$$

Since $\langle \bar{v}_r^0 \rangle = 1$, $\forall \bar{r}$, the hierarchy of equations (17) is exactly solvable. It is easy to prove recursively that its solution $\langle \bar{v}_r^{2p} \rangle$ is a finite linear combination of power laws of \bar{r} . The coefficient \bar{d}_0 in Eq. (18) is a small expansion parameter ($\bar{d}_0 \ll 1$). The truncation of Eq. (18) at first-order $O((\bar{d}_0)^1)$ reads

$$\langle v_r^{2p} \rangle = \langle v_L^{2p} \rangle \left(\frac{r}{L}\right)^{\alpha_{2p}} - d_0 L \langle v_L^{2p-2} \rangle \frac{2p(2p-1)}{1 + \alpha_{2p-2} - \alpha_{2p}} \times \left(\left(\frac{r}{L}\right)^{1 + \alpha_{2p-2}} - \left(\frac{r}{L}\right)^{\alpha_{2p}} \right), \quad (19)$$

where the physical variables v_r and r were used for clarity. Figure 3 shows that Eq. (19) fits data well up to $2p = 8$ for scales larger than 50η .

The scale dependence of even-order structure functions $\langle v_r^{2p} \rangle$ is captured by a Fokker–Planck equation (11) with a linear drift term $D_1(v_r, r) = -v_r/(3r)$ and an even diffusion coefficient $D_2^{\text{even}}(v_r, r) = d_0 + d_2 v_r^2/r$. The analytic expression of $\langle v_r^{2p} \rangle$ is the sum of a finite number of power laws of r . It is interesting to note that: (i) the dominant term $[\propto r^{\alpha_{2p}}$ at order $O((\bar{d}_0)^0)$] does *not* reproduce experimental data (see Fig. 3); (ii) a simple scaling law reminiscent of Kolmogorov–Obukhov’s theory $[\langle v_r^{2p} \rangle \propto r^{\zeta_{2p}}, \zeta_{2p} = (\gamma + d_2)2p - d_2(2p)^2]$ corresponds to the hypothetical limit $d_0 \rightarrow 0, D_2^{\text{even}}(v_r, r) \approx d_2 v_r^2/r$.

C. Odd-order moments

Since analytic expressions of all even-order moments are already known, the inhomogeneous term on the right hand side of Eq. (13) is completely known when solving recursively for the odd-order moments $\langle \bar{v}_r^{2p+1} \rangle$. Using $\langle \bar{v}_r \rangle = 0$, $\forall \bar{r}$, and expressions (18), it is easy to show that Eq. (13) is exactly solvable for all odd orders $n = 2p + 1$, and that its solution is also a finite linear combination of power laws of \bar{r} with different exponents.

Let us now focus on the third-order moment $\langle v_r^3 \rangle$. Since $\alpha_3 \approx 1$, the dominant term of the solution of (13) is linear, $\langle v_r^3 \rangle = \langle v_L^3 \rangle (r/L)$, in agreement with Kolmogorov’s four-fifths law. However, Fig. 4 shows that this linear behavior reproduces only the main slope observed in log–log scale: the discrepancy is of the order of 10% in relative value. The “inertial range” of this flow corresponds to $\langle v_r^3 \rangle \approx -0.6(\epsilon)r$, instead of the theoretical prediction $\langle v_r^3 \rangle = -0.8(\epsilon)r$. Indeed, the presence of corrections to the four-fifths law at experimentally accessible Reynolds numbers is a well-documented fact.¹⁰ Including subdominant contributions does *not* yield a better agreement with data: the inhomogeneous term on the right hand side of Eq. (13) is negligible ($\bar{d}_1 \approx 4\bar{d}_3, \bar{r} \leq 1$ and $\langle \bar{v}_{\bar{r}=1}^4 \rangle \approx 3$). The leading correction to the Gaussian approximation stems from the third-order Kramers–Moyal coefficient $D_3 \approx \gamma_3 v_r/r^3$, lead-

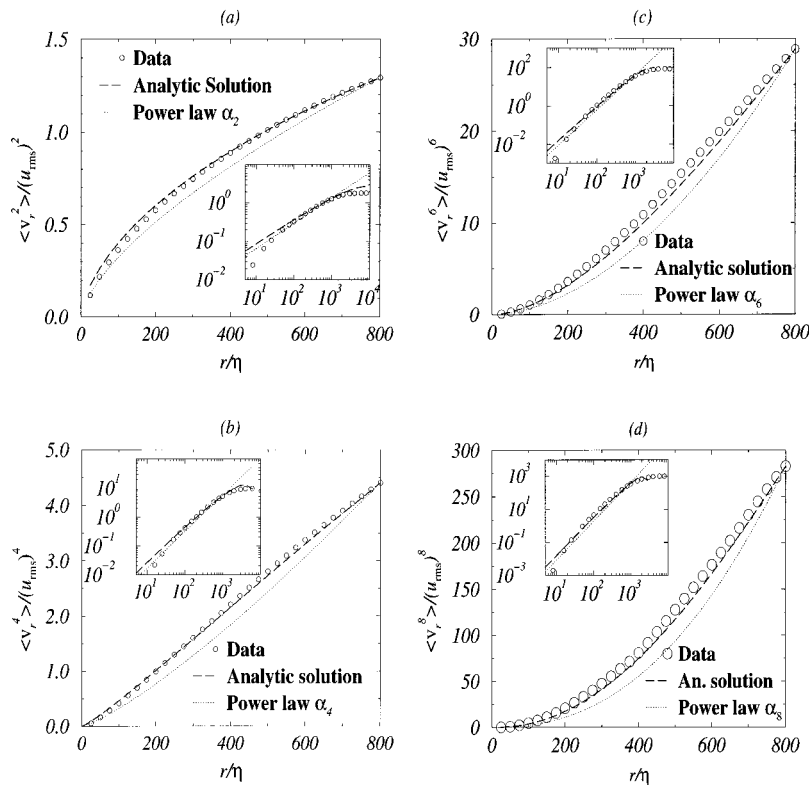


FIG. 3. Even-order dimensionless structure functions $\langle v_r^{2p} \rangle / (u_{rms})^{2p}$ vs r/η . (a) The second-order structure function (symbols) is compared to the analytic solution (19) (dashed line, $\bar{d}_0=0.09$, $\alpha_2=0.66$), and to a power law $\langle v_r^2 \rangle = \langle v_L^2 \rangle (r/L)^{\alpha_2}$ (dotted line, $\alpha_2=0.66$). The size of symbols gives the statistical error bar in the main (lin–lin) graph. The inset gives the same plot in log–log scale, for $\eta/2 \leq r \leq 800\eta = 5L$. (b) Fourth-order structure function ($\alpha_4=1.26$). (c) Sixth-order structure function ($\alpha_6=1.83$). (d) Eighth-order structure function ($\alpha_8=2.35$).

ing to the additional term $n(n-1)(n-2)\gamma_3 \langle \bar{v}_r^{n-2} \rangle / \bar{r}$ on the right-hand side of Eq. (13). This term vanishes for $n=3$: a detailed treatment of the non-Gaussian features of the random force is pointless.

Analysis of the fifth-order moment leads to similar observations (see Fig. 4): Equation (13) yields the dominant behavior of $\langle v_r^5 \rangle$, but not the curvature observed in a log–log plot, even when the non-Gaussian statistics of $\xi(r)$ is taken into account. We also checked that agreement between the analytic solution of Eq. (13) and data is only qualitative for higher odd-order moments. This may be due to the increased numerical difficulty involved in measuring accurately odd contributions to the diffusion coefficient.

VI. DISCUSSION

Our analysis shows that the scale dynamics of turbulent velocity increments can be described, for large enough scales, by the Langevin equation (2), with the drift and diffusion coefficients given by Eqs. (6) and (8) and a random force $\xi(r)$ defined by Eq. (9).

As already found in Refs. 3 and 4, we confirm that the random process v_r is Markovian. The cascade process is local in scale, since stochastic trajectories of v_r are uncorrelated over scales larger than the autocorrelation scale ρ of the random force $\xi(r)$, of the order of Kolmogorov’s scale η . The locality of the cascade, postulated in most statistical models of intermittency, is demonstrated experimentally and quantified. Further, we propose a physical explanation for this remarkable fact. The random force $\xi(r)$ is “rapid” compared to the “slow” stochastic variable v_r because the longitudinal velocity $u(x)$ is correlated over distances much larger than

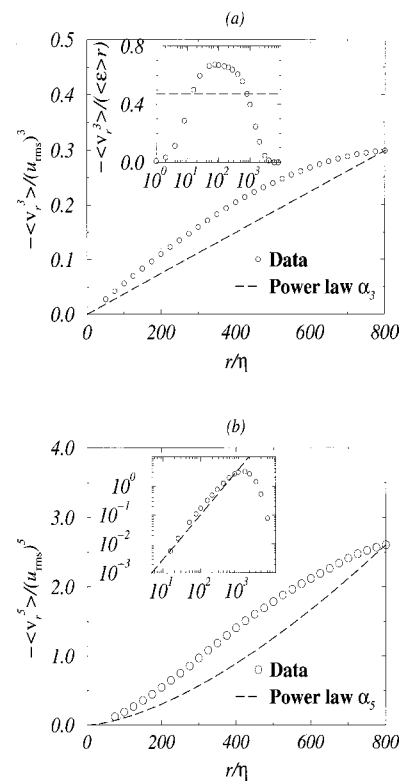


FIG. 4. Odd-order dimensionless structure functions $-\langle v_r^{2p+1} \rangle / (u_{rms})^{2p+1}$ vs r/η . (a) The third-order structure function (symbols) is compared to the power law $\langle v_r^3 \rangle = \langle v_L^3 \rangle (r/L)^{\alpha_3}$ (dashed line, $\alpha_3=1$). The size of the symbols gives the statistical error bar in the main (lin–lin) graph. The inset gives the ratio $-\langle v_r^3 \rangle / (\langle \epsilon \rangle r)$ as a function of scale. A constant value equal to 0.8 would correspond to Kolmogorov’s 4/5 law. (b) Fifth-order structure function ($\alpha_5=1.55$). The inset gives the same plot in log–log scale for $\eta/2 \leq r \leq 800\eta = 5L$.

the correlation length of its spatial derivative du/dx .

In order to check the consistency of our approach, a Gaussian approximation for the random force is made. The evolution equation for the pdf $P(v_r, r)$ becomes a Fokker–Planck equation. *Exact* solutions of the corresponding evolution equations for the structure functions $\langle v_r^n \rangle$ are obtained. For scales large compared to ρ (i.e., when the random force is uncorrelated), we checked that these solutions agree quantitatively with experimental data for even-order structure functions. However, the agreement is only qualitative for odd-order structure functions. The non-Gaussian character of the experimentally measured random force $\xi(r)$ can be ignored. It does not give rise to intermittent corrections to Kolmogorov’s scaling. This confirms that higher-order terms of the Kramers–Moyal expansion can be safely neglected.^{3,4}

Velocity increments obeying the Langevin equation (2) with the drift and diffusion coefficients (6) and (8) are characterized by an asymmetric, intermittent distribution. The exact solutions of (2) are linear combinations of power laws of the scale r . Their expressions provide a quantitative assessment of how inertial range behavior depends upon large scale fluctuations, through the integral scale L and the moments $\langle v_L^n \rangle$.

The physical picture which emerges here is the following: Kolmogorov’s scaling corresponds to a “classical path” for trajectories of $v_r: dv_r/dr = v_r/(3r)$, while finite Reynolds number corrections amount to fluctuations around this path. A characterization of the Reynolds number dependence of our measurements may help to substantiate this conjecture, in particular if the diffusion coefficient is indeed a decreasing function of R_λ . It may also help uncover the physical meaning of the various coefficients we introduced. One would also like to know whether this analysis depends on the nature of the turbulent flow. These important questions are left for future study.

ACKNOWLEDGMENTS

P.M. acknowledges financial support from the Alexander von Humboldt Foundation. The authors are grateful to Rudolf Friedrich and Joachim Peinke for a kind introduction to the subject and many stimulating discussions, and to Christophe Baudet for his friendly support and for the quality of his experimental facility.

¹A. N. Kolmogorov, “The local structure of turbulence in incompressible viscous fluid for very large Reynolds numbers,” *Dokl. Akad. Nauk SSSR* **30**, 299 (1941); “Dissipation of energy in the locally isotropic turbulence,” **32**, 19 (1941).

²K. R. Sreenivasan and R. A. Antonia, “The phenomenology of small-scale turbulence,” *Annu. Rev. Fluid Mech.* **29**, 435 (1997).

³R. Friedrich and J. Peinke, “Statistical properties of a turbulent cascade,” *Physica D* **102**, 147 (1997); “Description of a turbulent cascade by a Fokker–Planck equation,” *Phys. Rev. Lett.* **78**, 863 (1997).

⁴R. Friedrich, J. Zeller, and J. Peinke, “A note on three-point statistics of velocity increments in turbulence,” *Europhys. Lett.* **41**, 153 (1998).

⁵A. M. Polyakov, “Turbulence without pressure,” *Phys. Rev. E* **52**, 6183 (1995); V. Yakhot, “Probability density and scaling exponents of the moments of longitudinal velocity differences in strong turbulence,” *ibid.* **57**, 1737 (1998); J. Davoudi and M. Reza Rahimi Tabar, “Theoretical model for the Kramers–Moyal description of turbulence cascades,” *Phys. Rev. Lett.* **82**, 1680 (1999).

⁶P. Marcq and A. Naert, “A Langevin equation for the energy cascade in fully developed turbulence,” *Physica D* **124**, 368 (1998).

⁷C. Baudet, O. Michel, and W. J. Williams, “Detection of coherent vorticity structures using time-scale resolved acoustic spectroscopy,” *Physica D* **128**, 1 (1999).

⁸Y. Malécot, “Intermittence en turbulence 3D: Statistiques de la vitesse et de la vorticité,” *Doctoral thesis, Université de Grenoble, France, 1998.*

⁹N. G. van Kampen, *Stochastic Processes in Physics and Chemistry* (North-Holland, Amsterdam, 1992).

¹⁰E. Lindborg, “Correction to the four-fifths law due to variations of the dissipation,” *Phys. Fluids* **11**, 510 (1999); L. Danaila, F. Anselmetti, T. Zhou, and R. Antonia, “A generalization of Yaglom’s equation which accounts for the large-scale forcing in heated decaying turbulence,” *J. Fluid Mech.* **391**, 359 (1999).